Close accord on partial discharge diagnosis during voltage harmonics in electric motors fed by variable frequency drives

HASSAN, Waqar, AKMAL, Muhammad <http://orcid.org/0000-0002-3498-4146>, HUSSAIN, Ghulam Amjad, RAZA, Ali and SHAFIQ, Muhammad

Received: 17 March 2023 | Revised: 22 November 2023 | Accepted: 15 December 2023

IET Generation, Transmission & Distribution

DOI: 10.1049/gtd2.13089

The Institution of Engineering and Technology WILEY

ORIGINAL RESEARCH

Close accord on partial discharge diagnosis during voltage harmonics in electric motors fed by variable frequency drives

Waqar Hassan[1] | Muhammad Akmal[2] | Ghulam Amjad Hussain[3] | Ali Raza[4] | Muhammad Shafiq[5]

[1]Institute of Power Engineering (IPE), Universiti Tenaga Nasional (UNITEN), Kajang, Malaysia

[2]Department of Engineering and Mathematics, Sheffield Hallam University, Sheffield, UK

[3]College of Engineering and Applied Sciences, American University of Kuwait, Salmiya, Kuwait

[4]Department of Electrical Engineering, University of Engineering and Technology, Lahore, Pakistan

[5]Center for Advanced Power Systems, Florida State University, Tallahassee, Florida, USA

Correspondence
Muhammad Akmal, Department of Engineering and Mathematics, Sheffield Hallam University, Sheffield S1 1WB, UK.
Email: m.akmal@shu.ac.uk

Abstract

Partial discharge (PD) diagnostics test is a reliable solution for estimating insulation health conditions in power system components. During laboratory PD diagnostics, the effect of harmonic components in the voltage waveform generated by variable frequency drives (VFD) fed electric motors (EMs) is often overlooked. As VFD-fed EMs operate at low speeds, the harmonic concentration in the voltage increases. It has been found that PD activity in VFD-fed EM is significantly affected by the addition of harmonic components in the voltage, thus making it necessary to consider their impact when performing true PD diagnostics. This paper investigates the influence of voltage harmonic distortion produced in VFD-fed EM on PD severity and the subsequent insulation degradation. Eight VFD-fed EM are used to study the PD behaviour under different levels of harmonic pollution. The PD characteristics, such as inception voltage, pulse repetition rate, accumulated apparent charge, average discharge current, discharge power, and quadratic rate, are determined. Using probability distribution functions, PD activity and severity at various voltage harmonic levels are estimated. The proposed technique can be used to plan the maintenance activities that ensure the reliability for industrial applications dealing with the voltage harmonic distortion.

1 | INTRODUCTION

The variable frequency drives (VFD) fed electric motors (EMs) are widely used in automotive, ship, aviation, and manufacturing industries due to their cost efficiency, reliable speed control, lightweight, high specific power, and energy-saving capabilities [1–3]. However, when VFD-fed EMs are in operation, the harmonic components in the applied voltage waveform may develop, which could lead to premature insulation failure of the stator winding over time [4]. Therefore, online condition monitoring of VFD-fed EMs is essential to detect any preemptive winding insulation failure and plan regular maintenance activities [5, 6].

Partial discharges (PD) diagnostics test is a reliable method for estimating the health of stator insulation when conducting online condition-based monitoring and offline evaluation of VFD-fed EMs [7–9]. In laboratory-based studies, PD measurements are typically conducted using a sinusoidal waveform of the applied voltage. However, in field operations, variable speed operation of VFD-fed EM can produce several harmonic components, resulting in a distorted voltage waveform that can significantly affect PD activity in the winding insulation [5]. Therefore, a better understanding of harmonic distortion in the applied voltage waveform is essential for accurately assessing the severity of PD and establishing an effective maintenance scheduling strategy for stator insulation in EMs.

Previous studies have investigated the effects of VFD-fed EMs on PD behaviour and insulation degradation of stator windings [10–12]. For instance, Almeida et al. investigated technical and non-technical barriers (e.g. power quality and reliability issues) associated with the broader applications of VFD-fed EMs [13]. Also, the possible technical solutions to improve the performance of VFD-fed EMs based systems are discussed. In [14], Billard et al. studied the PD activity in EMs fed by inverter using a non-intrusive electromagnetic sensor. Furthermore, the experimental results revealed that PD activity in the stator

winding might lead to premature insulation failure. Florkowski et al. in [15] investigated the impact of harmonic pollution in the applied voltage waveform on PD behaviour and pattern evolution. Based on the experiments, the author observed that the harmonic distortion in the applied voltage significantly impacts PD intensity and maximum charge. In [16], Bahadoorsingh et al. studied the insulation characteristics of epoxy resin under harmonic distortion in the applied voltage waveform. It is also examined that the growth of an electric tree due to voltage harmonic distortion ultimately shortens the lifetime of the insulation. Hassan et al. explored the effect of harmonic contents in the applied voltage produced during the variable speed operation of EM on PD activity [5]. Also, mathematical modelling has been carried out to develop relationships between distortion and discharge parameters. Montanari et al. performed a comparative study investigating the influence of multi-level inverter supply and pure sine wave voltage on PD activity [17]. Furthermore, the aging estimation of the insulation in twisted wire pairs is also presented.

In summary, the existing literature has already studied the effect of specific voltage harmonic components on PD behaviour and winding insulation endurance in EM. However, there is a lack of knowledge about PD investigation under real harmonic regimes experienced during variable operating conditions of VFD-fed EM. This paper fills this gap by presenting the PD behaviour of VFD-fed EM under a real harmonic regime. Also, based on the experimental results, a method is proposed to establish the relationship between PD activity and severity with harmonic distortion produced in the VFD system.

This study aims to discuss the PD phenomenology, measurement techniques, and correlation with PD severity and the subsequent insulation degradation of EM insulation in a broad range of voltage harmonic distortion. For this purpose, the authors focused on low voltage (LV) VFD-fed EMs operating at different speed levels. Subsequently, PD activity is investigated by applying a constant voltage stress at speed ranging from 5% to 100% resulting total harmonic distortion in voltage (THD_V) up to 41.94% and waveshape parameter (K_s) up to 2.31, with detailed descriptions of these parameters provided in Section 4.2. Online PD measurements are performed under different voltage harmonic distortions by detecting a PD sweep signal of 20 ms. From the detected PD signal, several PD characteristic features, including PD inception voltage (PDIV), pulse repetition rate (n), accumulated apparent charge (q_a), average discharge current (I), discharge power (P), and quadratic rate (D), are evaluated. At a different level of harmonic distortion, the probability distribution functions of PD characteristic features are developed to infer statistical characteristics of PD data. With the help of an appropriate probability distribution function, the probability of PD activity and its severity at various voltage harmonic levels are estimated.

The rest of the paper is structured in the following way: Section 2 outlines the methodology used in this study. Section 3 explains the experimental setup, test object, and procedure for online PD measurement. In Section 4, the effects of variable speed operations of VFD-fed EM on voltage harmonics and characterization of the harmonic distortion are discussed. Section 5 presents the PD measurements and experimental results. Section 6 provides the probability of PD activity and estimation of PD severity. Finally, Section 7 summarizes the conclusions of this research.

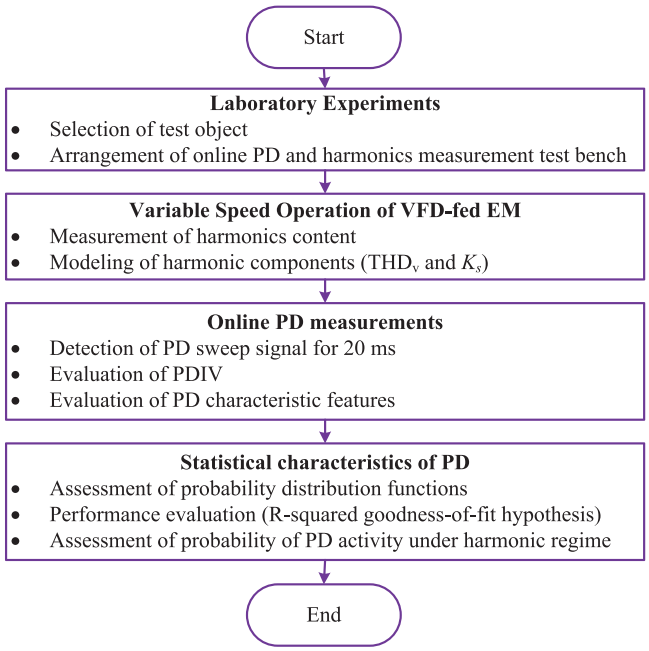

FIGURE 1 Methodology for analysing the impact of voltage harmonic distortion on Partial Discharge (PD) severity in Variable Frequency Drives fed Electric Motors.

2 | METHODOLOGY

Figure 1 illustrates the steps taken to investigate the influence of voltage harmonic distortion produced in VFD-fed EM on PD severity and the subsequent insulation degradation. The process is outlined as follows:

1. In the laboratory, a 12-pulse VFD and eight LV EMs having random wound stators with organic insulation are chosen for the experiment. A test bench for online PD measurement is set up to study the PD activity with different voltage harmonic distortion levels by recording the PD sweep signals of 20 ms. Both the 5th and 7th harmonic components are generated during the operation of 12-pulse VFD [4]. Additionally, the concentration of these harmonic components in the applied voltage waveform increases when the speed of VFD slows down. Therefore, a non-intrusive testing technique is used to evaluate the effect of variable speed operation of VFD-fed EMs on THD_v and K_s of the applied voltage.
2. At different levels of THD_V and K_s of the applied voltage, online PD measurements in VFD-fed EMs are conducted, and various PD features are assessed, which can be used to determine the extent of PD under varying levels of harmonic distortion.

3. Several probability distribution functions of PD characteristic features are evaluated to determine the statistical characteristics of PD data. Finally, the goodness-of-fit hypothesis is used to determine which probability distribution function best describes the probability of PD activity and associated severity level under various levels of voltage harmonic distortion.
4. This experimental work detected 350 PD sweep signals at different THD_V and K_s values of the applied voltage to obtain reliable results. This study is beneficial in demonstrating the PD activity under various levels of voltage harmonic distortion experienced by VFD-fed EMs during operation.

3 | LABORATORY EXPERIMENTS

In this section, the setup of an online PD experiment in a laboratory environment, the selection of VFD-fed EMs as the test object, and the procedure for PD diagnostics are described.

3.1 | Experimental setup

This laboratory-based online PD experimental setup comprises a 15-kVA adjustable three-phase AC power supply source (380–690 V) connected to VFD-fed EM. The EM is connected to VFD via a 1-m long, 10-mm diameter, single core flexible shielded power cable. The voltage harmonics in the power supply source are carefully analysed and found to be minimal (THD_V is less than 4%), making it effectively harmonic-free.

It is important to highlight that an increased cable length may trigger the voltage reflection phenomenon, which is harmful in VFD-fed EMs and results in overvoltage at the motor terminals [18]. In three-phase VFD-fed EMs system, PD measurements are also influenced by crosstalk phenomena, which result in interference between different phases of the EM [19]. The proper selection of VFD with features designed to reduce crosstalk, such as advanced PWM algorithms and filtering options, is essential. To reduce the impact of both voltage reflection and crosstalk phenomenon in VFD-fed EM system, a careful consideration of cable length and its characteristics can be effective. Furthermore, it is essential to consider the selection of switching speed (dv/dt) of PWM pulses. Despite several advantages, the high dv/dt causes a non-uniform distribution of voltage among the motor windings, therefore placing additional stress on the insulation of these initial winding turns [20]. To reduce the impact of voltage reflection phenomenon and overvoltage at the motor terminal, both low switching frequency (4 kHz) and low dv/dt (800 V/μs) of the drive is selected.

Figure 2 presents the experimental setup (schematic diagram and physical image) established to conduct online PD measurements. A power quality analyser is connected to VFD-fed EMs to assess the voltage harmonics during variable speed operations. The applied voltage is a line-to-line voltage that is supplied to VFD-fed EM system and recorded at the point of common coupling. A coupling capacitor (10 nF) is connected to one terminal of the EM, which served as a PD sensor and transferred

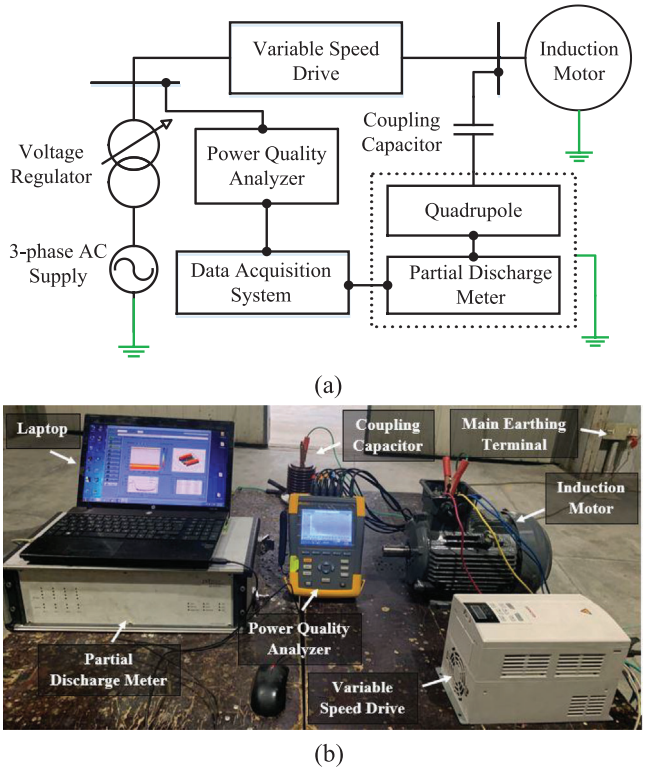

FIGURE 2 (a) Block diagram and (b) photograph show the experimental test setup developed in the laboratory for online partial discharge diagnostics.

the PD current pulses to the quadrupole. The quadrupole then converted these current pulses into voltage signals, providing the PD voltage signal to the PD detector. A data acquisition device is connected to the PD detector, translating the analogue PD signals into digital samples. The PD diagnostics tests are performed in accordance with the IEC 60034-27 Standard [9]. For the purpose of minimizing the attenuation of the captured signal, the PD detection system is tuned to a frequency of 1 MHz, adjusting the minimum values of linear error (less than 0.2 pC) and basic noise level (less than 0.1 dB). The calibration of the PD experimental test setup is carried out as per the IEC 60270 standard [21].

3.2 | Specification of test object

In this experimental study, a total of eight identical EMs is used. Table 1 presents the detailed technical specification of 12-pulse VFD and the EM used in the PD diagnostics.

Figure 3 presents the typical topology of 12-pulse VFD system. A standard 12-pulse VFD consists of several components, including a phase-shifting isolation transformer, rectifier, DC link, and inverter. The isolation transformer achieves dual outputs by transforming a three-phase AC power supply into a six-phase AC power supply. The rectifier consists of two sets of three-phase parallel six-diode bridges that facilitate the conversion of three-phase AC current into DC current. Before supplying to the inverter, the DC link voltage is passed through

TABLE 1 Technical specifications of variable frequency drive and electric motors used in the partial discharge diagnostics.

Description	Specification
Variable frequency drive (VFD)	Rated voltage: 380–690 V, 12 pulse, rated power: 7.5 kW, switching freq.: 4 kHz, switching speed: 800 V/μs, control mode: Scalar frequency, no. of phases: 3, PWM strategy: sinusoidal PWM, insulation class: F (155°C), input frequency: 50 Hz, output frequency: 5–50 Hz, brand: ABB
Induction motor	Rated voltage: 380–690 V, rated power: 5.5 kW, no. of phases: 3, rated current: 9.2 A, insulation class: F (155°C), no. of poles: 4, ingress protection (IP)−55, power factor (cos θ): 0.85, rated efficiency: 96%, input frequency: 50 Hz, connection: delta, brand: ABB

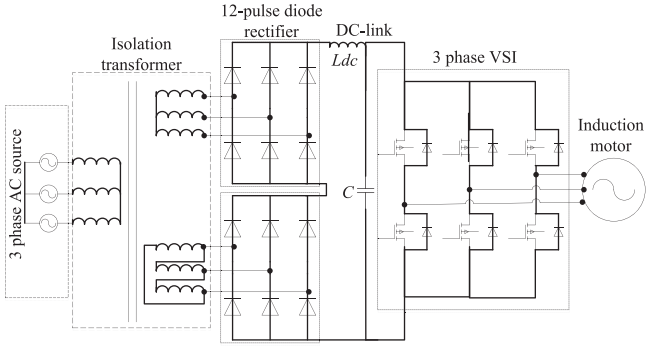

FIGURE 3 Common topology of variable frequency drive system.

an *LC* filter. The frequency of the output power supplied to the EM is controlled through the inverter timing [28].

3.3 | PD diagnostics procedure

This study used two sets of experiments to estimate the PD severity and calculation of PD characteristic parameters.

During the first set of experiments, the VFD is manually adjusted to set the operating speed of the EM at 100% of the designed speed. Based on our previous experimental results [4], the THD_V calculated at this speed is approximately 4.5%, meeting the standards [22], and a nearly sinusoidal waveform of voltage was produced. To ensure thermal stability, the VFD-fed EM is operated at this speed for 10–15 min. In certain situations, achieving thermal stability might require a longer duration (e.g. more than 30 min), particularly when dealing with larger motors or specific operating conditions. Following this, the PDIV at 100% operating speed is examined by slowly increasing the applied voltage. Subsequently, the operating speed is adjusted in small decrements from 100% to 5%, and experiments are repeated to assess the PDIV at different speed levels.

In the second set of experiments, the effects of voltage harmonic distortion produced during the variable speed operation of VFD-fed EM on PD activity are studied by assessing the

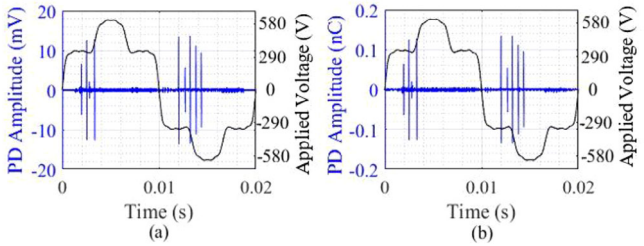

FIGURE 4 Partial Discharge sweep signal recorded at 41% operation speed, with $K_s = 1.73$, and $THD_V = 24.6\%$ (a) U_a (t_i) and U_{pd} (t_i) in mV, (b) U_a (t_i) and q_i in nC.

PD characteristic features. To achieve this, a voltage equal to PDIV value observed during 100% operating speed, is applied to the VFD-fed EM and PD activity is examined at this voltage under different speed levels ranging from 5% to 100%. At each operating speed, the harmonic distortion in the applied voltage waveform is recorded, and PD measurements are performed. The highest rank of the harmonics in the applied voltage waveform considered in this study is 25th.

Figure 4 provides a visual representation of a typical applied voltage waveform with harmonic distortion (black line) and its corresponding PD signal at an operating speed of 41% and THD_V of 24.6%. The PD signal in Figure 4a is shown as a blue line with its amplitude calibrated in mV, denoted by $V_{pd}(t_i)$. The same applied voltage waveform and PD signal in Figure 4b is calibrated in nC, denoted by q_i. The q_i is determined as:

$$q_i = C \times V_{pd}(t_i) \tag{1}$$

In Equation (1), C stands for the coupling capacitance and t_i is the sampling instant. With the PD signals obtained at different levels of voltage harmonics, several PD characteristic features such as q_a, m, I, P, and D can be determined to evaluate the impact of voltage harmonics distortion on the likelihood of PD activity in VFD-fed EM. The exact process for assessing PD characteristic features has already been outlined in [23].

4 | EFFECT OF VARIABLE OPERATING CONDITIONS OF VFD-FED EM ON HARMONICS

The variable speed operation of VFD-fed EM leads to the production of voltage harmonics which have a substantial impact on PD activity in the winding insulation. Therefore, it is essential to assess the level of voltage harmonic distortion in this type of EM prior to conducting PD diagnostics.

4.1 | Variable speed operation of VFD-fed EMs

In industrial applications, VFD are commonly used to control the EM speed and improve the energy efficiency. However,

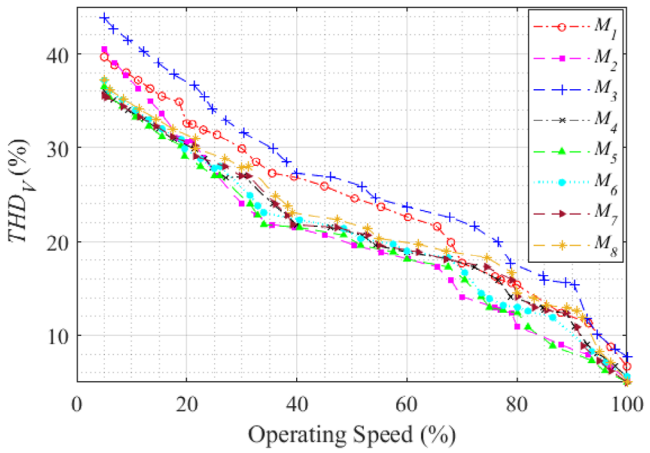

FIGURE 5 Relation between the speed ratio and Total Harmonic Distortion (THD_v) for eight Variable Frequency Drive fed Electric Motors (M-1 to M-8).

harmonics are produced in VFD due to the pulse width modulation (PWM) technique used in their operation, which is quantified by THD_V [24, 25]. The concentration of harmonics increases when VFD is operated at low speeds. Figure 5 presents the relationship between THD_V and operating speed for eight VFD-fed EMs observed during the experiments. It can be seen that the lower the operating speed, the higher the THD_V level.

4.2 | Characterization of harmonic distortion

Typically, the voltage harmonic distortion can be characterized using several parameters [16, 26]. These parameters include:

4.2.1 | THD_V rate

THD_V rate is an important measure for assessing the harmonic distortion in the voltage waveform [4], which can be calculated using Equation (2).

$$THD_V \quad (\%) = \sqrt{\sum_{n=2}^{N} \left(\frac{V_n}{V_1}\right)^2} \times 100 \tag{2}$$

where N represents the highest voltage harmonic order taken into account, n represents the specific voltage harmonic order, and V_n and V_1 are the rms values of nth order of voltage harmonic components and the fundamental voltage, respectively.

4.2.2 | Waveshape parameters (K_s and K_f)

Both K_s and K_f determine the steepness of the derivative of the resulting voltage waveform, which can contain harmonic distortion. The Fourier decomposition of this waveform is given by (3).

$$V\ (t) = \sum_{n=1}^{N} V_n\ \sin\left(n\omega_1 t + \psi_n\right) \tag{3}$$

where ω_1 is the angular frequency of the sinusoidal voltage waveform and ψ_n is the phase shift of the concerned harmonic order. From (3), the slope of the waveform is given as:

$$\left(\frac{dV\ (t)}{dt}\right)_{rms} = \frac{\omega_1}{\sqrt{2}} \sqrt{\sum_{n\,=\,1}^{N} n^2 V_n^2} \tag{4}$$

The slope of the fundamental applied voltage waveform is given as:

$$\left(\frac{dV}{dt}\right)_{rms} = \frac{\omega_1}{\sqrt{2}}\ V_1 \tag{5}$$

The value of K_f is calculated by dividing (4) with rms values of the derivative of sinusoidal voltage waveform, with the same value of fundamental component in the distorted voltage waveform, as given by (6):

$$K_f = \sqrt{\sum_{n=1}^{N} n^2 \alpha_n^2} \tag{6}$$

where

$$\alpha_n = \frac{V_n}{V_1} \tag{7}$$

K_s is given by (8)

$$K_s = \frac{\omega_1}{\omega_0} \times K_f \tag{8}$$

where ω_0 is the angular frequency of the fundamental voltage waveform and ω_1 is the angular frequency of 50 Hz voltage waveform. Also, the ratio of ω_1 and ω_0 is equal to 1, meaning that both Equations (6) and (7) are the same since ω_0 is equal to 50 Hz.

4.2.3 | Peak modification factor (K_p)

K_p is also known as peak parameter, and is calculated as:

$$K_p = \frac{V_{np}}{V_{1p}} \tag{9}$$

where V_{np} and V_{1p} represent the peak values of composite voltage waveform and fundamental voltage waveform, respectively.

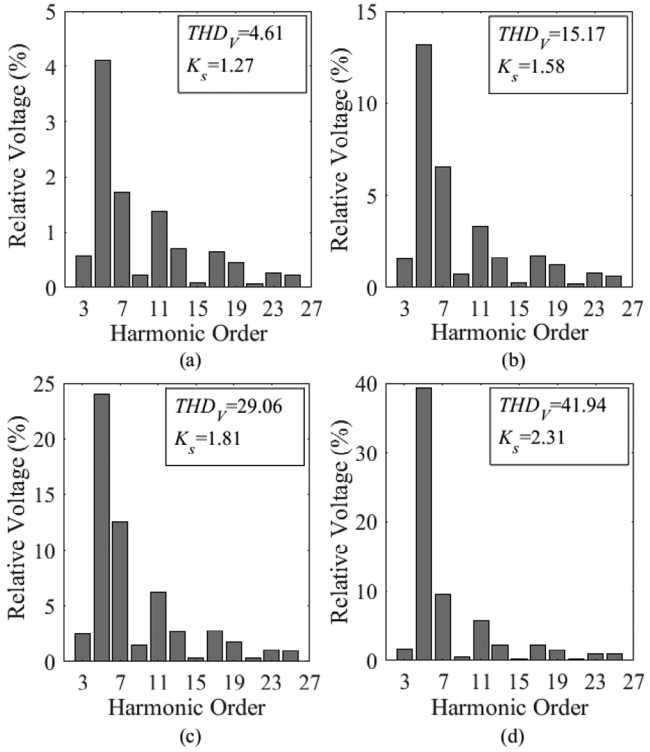

FIGURE 6 Harmonic spectrum of applied voltage waveform at an operating speed (a) 100%, (b) 71%, (c) 22%, and (d) 5%.

4.2.4 | RMS parameter (K_{rms}): K_{rms} is determined using (10)

$$K_{rms} = \frac{V_{nrms}}{V_{1rms}} \tag{10}$$

where V_{nrms} and V_{1rms} represent the rms values of composite voltage waveform and fundamental voltage waveform, respectively. In this study, THD_V and K_s are utilized to analyse the harmonic distortion in the applied voltage waveform.

4.3 | Investigation of applied voltage waveform

When VFD-fed EMs is operated at different speeds, the applied voltage waveform is captured using power quality analyser and harmonic components associated to a specific speed are modelled. It is observed that the decrease in the operating speed causes an increase in both THD_V and K_s, as witnessed in Figure 6. From Figure 6, when operating speed of EM is 100%, both THD_V and K_s are 4.61% and 1.27, respectively. By reducing the operating speed from 100% to 5%, both THD_V and K_s significantly raised up to 41.94% and 2.31, respectively. For each voltage waveform, the test is successively performed for five minutes, and PD activity is investigated. To eliminate the effect of preceding voltage waveform, each successive test is performed without disconnecting the applied voltage source.

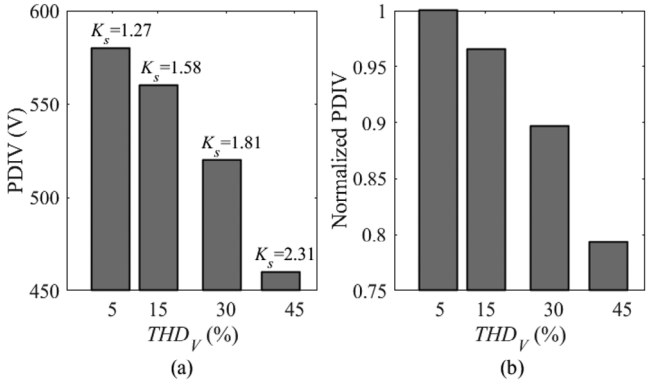

FIGURE 7 (a) Partial discharge inception voltage (PDIV) and (b) normalized PDIV calculated at different levels of total harmonic distortion in voltage (THD_V).

5 | EXPERIMENTAL RESULTS AND DISCUSSIONS

This section presents the PD measurements conducted online to evaluate the PDIV and PD characteristics under varying levels of voltage harmonic concentration.

5.1 | Partial discharge inception voltage (PDIV)

The PD activity is studied under different voltage harmonics by measuring the *PDIV*. For each THD_V level, the experiment is carried out ten times and the average value of PDIV is calculated. The results of PDIV at different THD_V levels are displayed in Figure 7. From Figure 7a, the presence of harmonic components in the applied voltage waveform can be seen to reduce the PDIV. This reduction is from 580 to 460 V when THD_V and K_s levels are increased from 4.61% to 41.94% and 1.27 to 2.31, respectively. The normalized PDIV at a given THD_V level, represented by $U_{i,N}(THD_V)$, is then calculated to compare the value of PDIV reduced due to the presence of harmonic components in the applied voltage waveform, as expressed by (11).

$$U_{i,N}\ (THD_V) = \frac{U_i\,(THD_V)}{U_i\,(f)} \tag{11}$$

where $U_i(THD_V)$ and $U_i(f)$ represent the average values of PDIV calculated at specific THD_V level and at reference THD_V level, respectively. Figure 7b presents the results of normalization. From Figure 7b, it can be observed that the increase in THD_V level from 4.61% to 41.94% causes to reduce the $U_{i,N}(THD_V)$ to 0.793.

5.2 | Online partial discharge diagnostics

The online PD measurements are conducted at different levels of voltage harmonics produced in VFD-fed EMs, and results

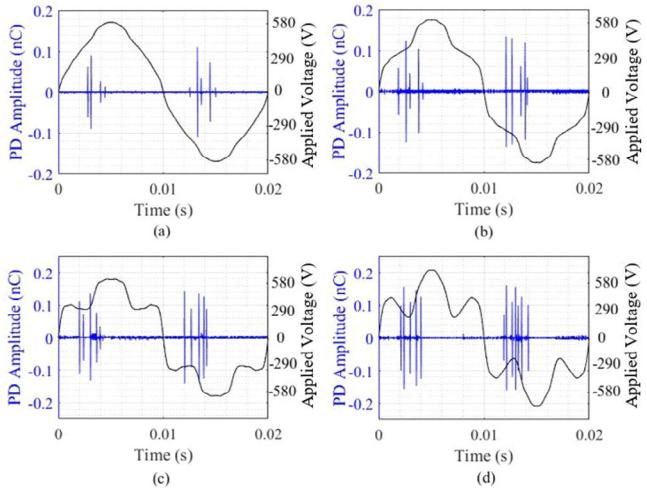

FIGURE 8 Partial discharge activity captured at various levels of total harmonic distortion in voltage (THD_V) and waveshape parameter (K_s) (a) 4.61% and 1.27, (b) 15.17% and 1.58, (c) 29.06% and 1.81, and (d) 41.94%, and 2.31, respectively.

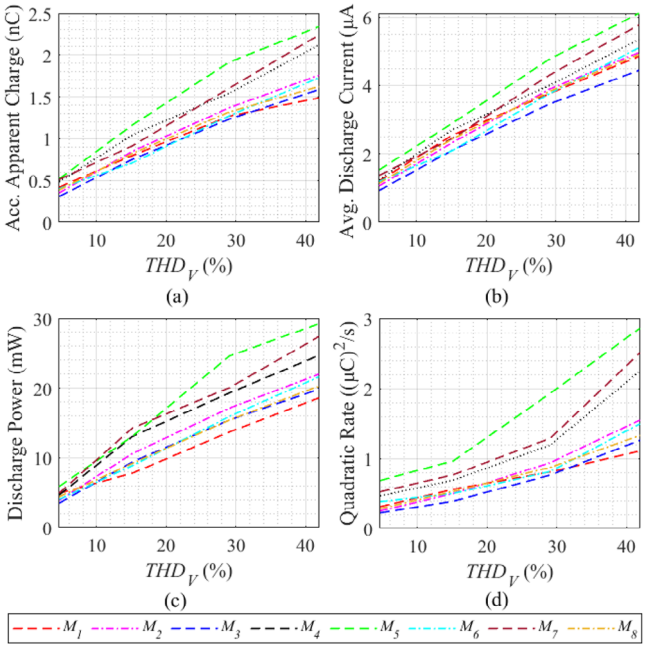

FIGURE 9 PD characteristic features identified for eight VFD-fed EMs under a range of voltage harmonic distortion (a) q_a, (b) I, (c) P, and (d) D.

are presented in Figure 8. For each THD_V level, the test is conducted 10 times and the trigger level for all the measurements is adjusted as 10 pC. Based on the PD sweep signal captured for reference time (T_r) equal to 20 ms, PD activity is investigated by calculating the average PD pulse amplitude (q_i) and pulse repetition rate (m).

In the beginning, the VFD-fed EMs are operated at designed speed (e.g. equal to 100%), and PD measurements are carried out at nearly sinusoidal waveform of the applied voltage $THD_V = 4.61\%$ and $K_s = 1.27$, the results are outlined in Figure 8a. From Figure 8a, at minimum values of THD_V and K_s, both q_i and m determined from the captures PD signals are also minimum. For T_r equal to 20 ms, only a few PD pulses (30 s^{-1}) with noticeable values of q_i (0.047 nC) are observed.

The operating speed of VFD-fed EMs is gradually reduced to 71%, 22%, and 5%, and PD measurements are carried out at higher levels of THD_V and K_s. Figure 8b–d presents the PD measurements carried out at THD_V and K_s levels up to 15.17% and 1.58, 29.06% and 1.81, and 41.94%, and 2.31, respectively. From Figure 8b, it can be observed that both q_i and m evaluated at 15.17% THD_V and 1.58 K_s are (50 s^{-1}) and (0.0611 nC), slightly higher than the both values observed in Figure 8a. Similarly, that both q_i and m evaluated at 29.06% THD_V and 1.81 K_s and are (55 s^{-1}) and (0.102 nC), as witnessed in Figure 8c. At 41.94% THD_V and 2.31 K_s, PD signals captured for 20 ms contain the highest values of both m and q_i (e.g. 60 s^{-1} and 0.12 nC), respectively. Therefore, by increasing THD_V (from 4.61% to 41.94%) and K_s (from 1.27 to 2.31), both m and q_i increased up to 100% and 155%, respectively.

5.3 | Evaluation of PD characteristic features

At different levels of voltage harmonic distortion, the PD characteristic features including q_a, I, P, and D are evaluated, results are depicted in Figure 9. From Figure 9, it can be inferred that the increase in the level of voltage harmonic distortion causes a significant increase in PD characteristic features. For instance, the increase in THD_V level from 4.61% to 41.94% and K_s level from 1.27 to 2.31 cause an increase in q_a up to 4.3 times, I up to 4.5 times, P up to 4.9 times, and D up to 5.1 times. Therefore, it can be inferred that the increase in PD characteristic features at high level of voltage distortion amplified the PD severity level, and ultimately, the risk of insulation failure in VFD-fed EMs is increased.

5.4 | Discussions

The introduction of harmonic components in the applied voltage waveform leads to a noticeable increase in PD activity (e.g. PDIV decreases and the values of PD characteristic features increase). This change in PD behaviour when VFD-fed EMs are operated can be explained in three different ways.

In the first way, the addition of harmonic components to the applied voltage increases the peak amplitude of the voltage waveform, resulting in extended PD activity at higher voltage amplitudes.

The decrease in the operating speed of VFD-fed EM introduces additional current harmonic distortion in the sinusoidal current waveform and reduces the cooling airflow (in self-cooled motors), which subsequently rises the stator winding temperature [13]. When at higher temperatures, electrons absorb thermal energy, reduces the relative air density of electrons, this leads to increase the electron mean free path. Therefore, the electrons absorb more energy and travel a greater distance between two collisions, leading to electric discharge.

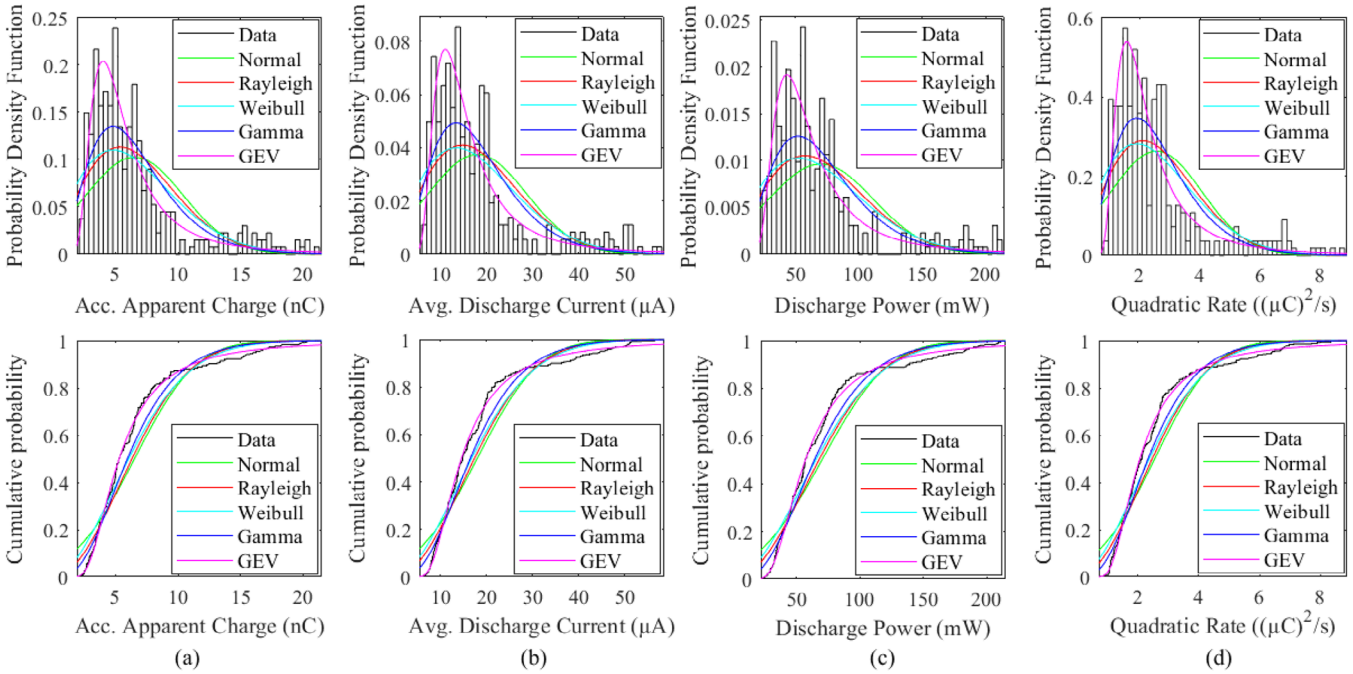

FIGURE 10 Example of probability of density function (PDF) and cumulative distribution function (CDF) for data fitting of partial discharge (PD) features at 4.61% THD_V and 1.27 K_s (a) q_a, (b) I, (c) P, and (d) D.

In the third way, when the harmonic distortion of the applied voltage waveform is increased, the equilibrium temperature of the stator winding in EMs rises [27], reducing the amount of energy that needs to be supplied by bombarding electrons. This makes PD more energetic and powerful at high values of voltage harmonics.

6 | ESTIMATION OF PARTIAL DISCHARGE SEVERITY

The PD severity in the VFD-fed EMs can be estimated based on the PD characteristic features (e.g. q_a, I, P, and D) evaluated at a certain voltage harmonic distortion level. To do this, various probability distribution functions are used to create probability density functions (PDFs) and cumulative distribution functions (CDFs) with the PD characteristic features data at different voltage harmonic distortion levels. At a specific harmonic level, 350 data samples of PD sweep signal were captured and corresponding values of q_a, I, P, and D are determined. The PD measurements are ignored for PD amplitude values lower than 10 pC. Accordingly, PDF and CDF using probability distribution functions (e.g. Normal, Rayleigh, Weibull, Gamma, and Generalized extreme value (GEV) are employed for the fitting of PD data. For instance, Figure 10 presents the plot of PDF and CDF for data fitting of q_a, I, P, and D at 4.61% THD_V and 1.27 K_s. An appropriate distribution function is discovered by employing the distribution fitting tools.

The Generalized extreme value (GEV) distribution, introduced by Jenkinson in 1955, is used to describe the probability distribution function of standardized maxima or minima. The GEV distribution is a three-parameter function, consisting of shape parameter (ξ), location parameter (μ), and scale parameter (σ). Based on the shape parameter (ξ), GEV probability distribution family is further divided into three types such as Weibull distribution when $\xi < 0$, Freshet distribution when $\xi > 0$, and Gumbel distribution when $\xi = 0$ [28].

TABLE 2 Results of R-square hypothesis test (coefficient of determination).

PD feature	Normal	Rayleigh	Weibull	Gamma	GEV
q_a	0.6752	0.6997	0.7265	0.7817	0.9654
I	0.6617	0.6698	0.6919	0.7854	0.9612
P	0.6742	0.7141	0.7401	0.7765	0.9599
D	0.6887	0.7021	0.7511	0.7656	0.9432

The R-squared (R^2) goodness-of-fit hypothesis is conducted to determine which of the five probability distribution functions best fit the PD characteristic features. The results of this hypothesis are presented in Table 2, and it is found that GEV yields the highest coefficient of determination in three out of four PD characteristic features. Consequently, GEV was chosen to estimate the probability of PD activity under voltage harmonic concentration

Using three parameters GEV distribution function, PDF for PD characteristic features is given by (12) [29].

$$f(x) = \frac{1}{\sigma}(1 + \mathfrak{F}x)^{\frac{-1}{\mathfrak{F}}-1} \exp -(1 + \mathfrak{F}x)^{\frac{-1}{\mathfrak{F}}} \qquad (12)$$

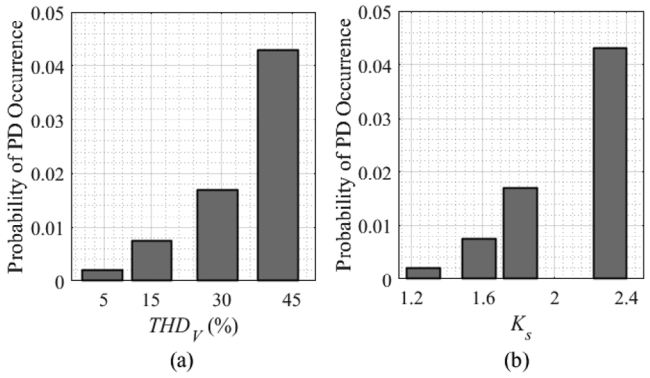

FIGURE 11 Estimated likelihood of PD activity occurring under different harmonic compositions.

where

$$x = \frac{z - \mu}{\sigma}, x > \mu - \frac{\sigma}{\mathfrak{F}} \text{for} \mathfrak{F} > 0 \tag{13}$$

By integrating (12), the CDF $P_c(x; \xi)$ is given by (14).

$$P_c\left(x;\xi\right) = \exp - (1 + \mathfrak{F}x)^{\frac{-1}{\mathfrak{F}}} \tag{14}$$

For estimating the PD severity at a specific voltage harmonic distortion level, the PD characteristic features estimated at almost sinusoidal voltage waveform (4.61% THD_v and 1.27 K_s) are taken as the reference values (e.g. $q_{a,ref}$, I_{ref}, P_{ref}, and D_{ref}). Therefore, the probability of occurrence ($P_o(x)$) of PD characteristic features (e.g. q_a, I, P, and D), that characterizes the PD severity, at a specific harmonic level greater than or equal to the PD characteristic features (I_{ref}, $q_{a,ref}$, D_{ref}, and P_{ref}) estimated at 4.61% THD_v and 1.27 K_s is given by (15).

$$P_o\ (x) = \ 1 - P_c\left(x;\xi\right) \tag{15}$$

Considering the combined influence of four PD characteristic features (e.g. q_a, I, P, and D), the average probability of occurrence of PD activity ($P_{o,a}$) at a specific voltage harmonics level is calculated using linearly distributed PD characteristic features.

$$P_{o,a} = q_{a,N}\frac{P_o\left(q_a\right)}{4} + I_N\frac{P_o\left(I\right)}{4} + P_N\frac{P_o\left(P\right)}{4} + D_N\frac{P_o\left(D\right)}{4} \tag{16}$$

where $q_{a,N}$, I_N, P_N, and D_N, represent the normalized values of I, q_a, D, and P calculated by (11). $P_o(I)$, $P_o(q_a)$, $P_o(D)$, and $P_o(P)$ represent the corresponding probability of occurrence of q_a, I, P, and D at specific harmonics level. Figure 11 presents the $P_{o,a}$ calculated at different levels of voltage harmonic distortion. From Figure 11, it was found that the increase in THD_V and K_s levels significantly increases the $P_{o,a}$, and PD severity in VFD-fed EMs is also increased.

Based on the estimated probability of occurrence of PD activity under different harmonic components, the assessment of PD severity is made by defining four different classes, as presented in Table 3. From Table 3, the severity levels are classified into negligible, low, medium, and high.

By employing online condition monitoring of VFD-fed EMs and determining machine-specific parameters for each insulation type (e.g. reference values of PD characteristic features), this technique serves as a diagnostic tool for assessing insulation quality throughout the motor's operational lifespan under varying harmonic concentrations. The asset managers can take remedial actions and schedule regular maintenance activities to ensure the healthy operation of VFD-fed EMs during voltage harmonic distortion. For instance, asset managers may follow the routine maintenance activities when PD severity level is negligible. Further increase in the PD severity from negligible to low level, the routine/normal maintenance period may be decreased. When PD severity is increased to medium level, EM is taken under observation. With further increase in the PD severity level from medium to high, a complete inspection of VFD-fed EM by a human expert is necessary to replace the required components. Furthermore, the increase in PD severity due to voltage harmonic components can be avoided either mitigating the harmonic components or implementing an optimum operation of VFD-fed EMs [4].

7 | CONCLUSIONS

This research investigated the effects of voltage harmonic distortion produced due to variable speed operation of VFD-fed EMs for estimating the PD severity.

The results suggested that the harmonic distortion has a significant impact on the PD severity, making reliable operation of VFD-fed EMs a challenge. The harmonic distortion parameters of the voltage waveform, K_s and THD_V, increased from 1.27 to 2.31 and 4.61% to 41.94%, respectively, during the experiments. These changes resulted in an increase in the values of PD characteristic features (q_a, I, P, D, and m) to 4.3 times, 4.5 times, 4.9

TABLE 3 Probability ranges and severity classes.

Level	Probability range	Severity class	Definition
(1) Negligible	$P_f \leq 10^{-3}$	Normal	No serious discharge occurs (Initial PD stage)
(2) Low	$10^{-3} < P_f \leq 5^{-3}$	Attention	Weak discharge pulses appear
(3) Medium	$5^{-3} < P_f \leq 5^{-1}$	Serious	PD pulses with significantly high amplitude appear
(4) High	$P_f \geq 5^{-1}$	Pre-breakdown	PD pulses with very high amplitude appear

times, 5.1 times, and 2 times, respectively. These increases in PD characteristic parameters lead to an increased PD severity level and, consequently, a higher risk of insulation failure. Therefore, it is essential to have a thorough understanding of harmonic content in order to properly assess the effect of PD activity on insulation health and avoid any misinterpretations of PD data.

By applying five different probability distribution functions, the likelihood of PD activity and its severity at different voltage harmonic levels are calculated. The R-squared goodness-of-fit hypothesis is applied to investigate which of the five probability distribution functions is most suitable for fitting the PD characteristic features. The results of the hypothesis, with GEV having the highest coefficient of determination for three out of four PD characteristics. Consequently, GEV is utilized to estimate the probability of PD activity under voltage harmonic concentration.

This technique can be used to plan maintenance and replacement activities, ensuring a reliable level of performance for different industrial applications of VFD-fed EMs dealing with voltage harmonic distortion, even those with different insulation types.

AUTHOR CONTRIBUTIONS

Waqar Hassan: Conceptualization; data curation; formal analysis; investigation; methodology; resources; writing—original draft. **Muhammad Akmal**: Formal analysis; investigation; methodology; supervision; writing—review and editing. **Ghulam Amjad Hussain**: Methodology; resources; supervision; writing—review and editing. **Ali Raza**: Methodology; resources; writing—review and editing. **Muhammad Shafiq**: Supervision; validation; writing—review and editing.

CONFLICT OF INTEREST STATEMENT

The authors declare no conflicts of interest.

FUNDING INFORMATION

This paper has not received any public funding.

DATA AVAILABILITY STATEMENT

The data that support the findings of this study are available from the first or corresponding author upon reasonable request.

ORCID

Waqar Hassan https://orcid.org/0000-0003-4115-9408
Muhammad Akmal https://orcid.org/0000-0002-3498-4146
Ghulam Amjad Hussain https://orcid.org/0000-0002-5161-7233
Ali Raza https://orcid.org/0000-0003-0947-3616
Muhammad Shafiq https://orcid.org/0000-0002-2272-0899

REFERENCES

1. Hughes, A., Drury, W.: Electric Motors and Drives: Fundamentals, Types and Applications. Newnes, Oxford (2013)
2. Stone, G.C., Sedding, H.G., Chan, C.: Experience with online partial-discharge measurement in high-voltage inverter-fed motors. IEEE Trans. Ind. Appl. 54(1), 866–872 (2018)
3. Wang, Y., Balachandran, T., Hoole, Y., Yin, Y., Haran, K.S.: Partial discharge investigation of form-wound electric machine winding for electric aircraft propulsion. IEEE Trans. Transp. Electrif. 6(4), 1638–1647 (2020)
4. Hassan, W., Mahmood, F., Akmal, M., Nasir, M.: Optimum operation of low voltage variable-frequency drives to improve the performance of heating, ventilation, and air conditioning chiller system. Int. Trans. Electr. Energy Syst. 30(9), e12481 (2020)
5. Hassan, W., Mahmood, F., Andreotti, A., Pagano, M., Ahmad, F.: Influence of voltage harmonics on partial discharge diagnostics in electric motors fed by variable-frequency drives. IEEE Trans. Ind. Electron. 69(10), 10605–10614 (2021)
6. Bucci, G., Ciancetta, F., Fiorucci, E., Ometto, A.: Uncertainty issues in direct and indirect efficiency determination for three-phase induction motors: Remarks about the IEC 60034-2-1 standard. IEEE Trans. Instrum. Meas. 65(12), 2701–2716 (2016)
7. Koltunowicz, W., et al.: Evaluation of stator winding insulation using a synchronous multi-channel PD technique. IEEE Trans. Dielectr. Electr. Insul. 27(6), 1889–1897 (2020)
8. IEC Standard 60034-27-1: Rotating electrical machines Part 27-1, Off-Line Partial Discharge Measurements on the Winding Insulation, International Electrotechnical Commission (2017)
9. IEC Standards 60034-27-2: Rotating electrical machines Part 27-2: On-line partial discharge measurements on the stator winding insulation of rotating electrical machines. International Electrotechnical Commission (2012)
10. Wang, P., Montanari, G.C., Cavallini, A.: Partial discharge phenomenology and induced aging behavior in rotating machines controlled by power electronics. IEEE Trans. Ind. Electron. 61(12), 7105–7112 (2014)
11. Montanari, G.C., Seri, P.: A partial discharge–based health index for rotating machine condition evaluation. IEEE Electr. Insul. Mag. 34(2), 17–23 (2018)
12. Yuen, K.K.-f., Chung, H.S.-h.: Use of synchronous modulation to recover energy gained from matching long cable in inverter-fed motor drives. IEEE Trans. Power Electron. 29(2), 883–893 (2013)
13. de Almeida, A.T., Ferreira, F.J., Both, D.: Technical and economical considerations in the application of variable-speed drives with electric motor systems. IEEE Trans. Ind. Appl. 41(1), 188–199 (2005)
14. Billard, T., Lebey, T., Fresnet, F.: Partial discharge in electric motor fed by a PWM inverter: Off-line and on-line detection. IEEE Trans. Dielectr. Electr. Insul. 21(3), 1235–1242 (2014)
15. Florkowski, M., Florkowska, B., Furgał, J., Zydron, P.: Impact of high voltage harmonics on interpretation of partial discharge patterns. IEEE Trans. Dielectr. Electr. Insul. 20(6), 2009–2016 (2013)
16. Bahadoorsingh, S., Rowland, S.: Investigating the impact of harmonics on the breakdown of epoxy resin through electrical tree growth. IEEE Trans. Dielectr. Electr. Insul. 17(5), 1576–1584 (2010)
17. Montanari, G.C., Seri, P.: The effect of inverter characteristics on partial discharge and life behavior of wire insulation. IEEE Electr. Insul. Mag. 34(2), 32–39 (2018)
18. Xu, Y., et al.: Impact of high switching speed and high switching frequency of wide-bandgap motor drives on electric machines. IEEE Access 9, 82866–82880 (2021)
19. Morya, A.K., et al.: Wide bandgap devices in AC electric drives: Opportunities and challenges. IEEE Trans. Transp. Electrif. 5(1), 3–20 (2019)
20. Guardado, J., Cornick, K.: The effect of coil parameters on the distribution of steep-fronted surges in machine windings. IEEE Trans. Energy Convers. 7(3), 552–559 (1992)
21. IEC Standard 60270: High-voltage test techniques: partial discharge measurements. International Electrotechnical Commission, pp. 13–31 (2000)
22. IEEE Standard, 519-2014, IEEE Recommended Practice and Requirements for Harmonic Control in Electric Power Systems, pp. 1–29 (2014)
23. Hassan, W., Hussain, G.A., Mahmood, F., Amin, S., Lehtonen, M.: Effects of environmental factors on partial discharge activity and estimation of insulation lifetime in electrical machines. IEEE Access 8, 108491–108502 (2020)

24. IEEE recommended practices and requirements for harmonic control in electrical power systems. In IEEE Std 519-1992, New York, NY, USA, pp. 1–112 (1993). https://doi.org/10.1109/IEEESTD.1993.114370
25. Lingom, P.M., Song-Manguelle, J., Betoka-Onyama, S.P., Nyobe-Yome, J.M., Doumbia, M.L.: A power quality assessment of electric submersible pumps fed by variable frequency drives under normal and failure modes. Energies 16(13), 5121 (2023)
26. Catterson, V.M., Bahadoorsingh, S., Rudd, S., McArthur, S.D., Rowland, S.M.: Identifying harmonic attributes from online partial discharge data. IEEE Trans. Power Delivery 26(3), 1811–1819 (2011)
27. Hassan, W., Hussain, G.A., Mahmood, F., Akmal, M.: Quantifying the probability of partial discharge in VFD fed electric motors under voltage harmonics concentration. In: 2022 20th International Conference on Harmonics and Quality of Power (ICHQP). Naples, Italy, pp. 1–6 (2022)
28. Bücher, A., Segers, J.: On the maximum likelihood estimator for the generalized extreme-value distribution. Extremes 20(4), 839–872 (2017)
29. Pinheiro, M., Grotjahn, R.: An introduction to extreme value statistics. Tutorial at University of California at Davis (2015), Available Online: https://grotjahn.ucdavis.edu/EWEs/extremes_primer_v9_22_15.pdf

How to cite this article: Hassan, W., Akmal, M., Hussain, G.A., Raza, A., Shafiq, M.: Close accord on partial discharge diagnosis during voltage harmonics in electric motors fed by variable frequency drives. IET Gener. Transm. Distrib. 1–11 (2023). https://doi.org/10.1049/gtd2.13089